

Supplemental Materials

Contents

1	Supplemental Tables	2
2	Supplemental Text	6
2.1	Key equations	6
2.2	Comparison to alternative synergy models	7
2.2.1	The Dose Equivalence Principle: Loewe and CI	7
2.2.2	The Multiplicative Survival Principle: Bliss and Effective Dose Model	8
2.2.3	ZIP	9
2.2.4	BRAID	9
2.2.5	Highest Single Agent (HSA)	9
2.2.6	Schindler 2D-Partial Differential Equation (PDE) Model	9
2.3	Sham Experiment	10
3	Derivation of generalized 2-dimensional hill equation	11
3.1	One-dimensional sigmoidal dose-response curve	11
3.2	Extending the mass action paradigm to simple four-state model assuming detailed balance	11
3.3	Four-state model with multiple steps between states	14
3.4	Generalized derivation without assuming detailed balance	16
4	Supplemental Bibliography	17

1 Supplemental Tables

Table S1: Annotation of parameters for the 2D Hill equation. Related to Figure 1, Figure S1.

U	Percent of unaffected cells
A_1, A_2	Percent of cells affected by drug 1 and drug 2, respectively.
$A_{1,2}$	Percent of cells affected by both drug 1 and drug 2.
d_1, d_2	Drug concentrations for drug pair
E_d	Measured DIP rate at (d_1, d_2)
C_1, C_2	EC_{50} for drugs 1 and 2 in isolation
r_x, r_{-x}	The forward and reverse transition rates between two states
h_1, h_2	Hill coefficients for dose response curves of drug 1 and 2 in isolation
E_0	The basal rate of proliferation in drug naive condition
E_1, E_2	E_{max} of drug 1 and 2 in isolation
E_3	E_{max} of the combination of drugs 1 and 2
α_1	Measure of how $[d_1]$ modulates the effective dose of $[d_2]$.
α_2	Measure of how $[d_2]$ modulates the effective dose of $[d_1]$.
β	Theoretical difference in maximal effect achievable with both drugs compared to the most efficacious drug alone (eq. 3)
β_{obs}	Observed difference in effect with both drugs at the maximum tested concentration as compared to either drug alone (eq. 4)

Table S2: Annotation of anti-cancer drugs used in NSCLC and BRAF-mutant melanoma screens with nominal target and target class. Related to Figure 2,3.

Class	Subclass	Drug	Tested Range	Nominal Target
NSCLC				
Epigenetic Regulators	BET	jq1	4.0uM-0.1nM,0nM	BET bromo-domain
	HDACi	abexinostat	0.3uM-0.8nM,0nM	HDAC
		entinostat	1.0uM-2.6nM,0nM	HDAC
		givinostat	10.0uM-41.1nM,0nM	HDAC
		m344	1.0uM-2.6nM,0nM	HDAC
		mocetinostat	0.3uM-0.8nM,0nM	HDAC
		panobinostat	0.4uM-0.0nM,0nM	HDAC
		pracinostat	10.0uM-41.1nM,0nM	HDAC
		quisinostat	1.0uM-2.6nM,0nM	HDAC
	TF	bazedoxifene	10.0uM-41.1nM,0nM	ER
		verteporfin	10.0uM-41.1nM,0nM	YAP
Kinases	ALK	ceritinib	4.0uM-0.1nM,0nM	ALK/IGF1R
		ensartinib	4.0uM-0.1nM,0nM	ALK
	AURK/CDKs	bml259	1.0uM-2.6nM,0nM	CDK
		zm447439	4.0uM-0.1nM,0nM	AURK
	MAPK/PI3K	dactolisib	4.0uM-0.1nM,0nM	PI3K/mTOR
		ly294002	10.0uM-41.1nM,0nM	PI3K
		rapamycin	0.3uM-0.8nM,0nM	mTOR
		sb253226	10.0uM-41.1nM,0nM	p38
		tak632	4.0uM-0.1nM,0nM	RAF
		trametinib	0.3uM-0.8nM,0nM	MEK
		u0126	10.0uM-41.1nM,0nM	MEK
		ulixertinib	4.0uM-0.1nM,0nM	ERK
	SFK	bosutinib	10.0uM-41.1nM,0nM	Bcr-ABL/SFK

Mitotic Checkpoint	DNA Syn/Dam	dasatinib	1.0uM-3.9nM,0nM	SFK
		pp2	10.0uM-41.1nM,0nM	SFK
		quercetin	10.0uM-41.1nM,0nM	SFK
		carmustine	10.0uM-41.1nM,0nM	DNA
	Protein Syn/Stab	methotrexate	4.0uM-0.1nM,0nM	DHFR
		olaparib	20.0uM-0.3nM,0nM	PARP
		carfilzomib	4.0uM-0.1nM,0nM	Proteasome
		harringtonine	10.0uM-41.1nM,0nM	Ribosomes
		mg132	4.0uM-0.1nM,0nM	Proteasome
	Tubulin	tanespimycin	4.0uM-0.1nM,0nM	HSP90
		cephalomannine	10.0uM-41.1nM,0nM	Microtubules
		docetaxel	0.3uM-0.8nM,0nM	Microtubules
		vindesine	0.3uM-0.8nM,0nM	Microtubules
		vinorelbine tartrate	10.0uM-41.1nM,0nM	Microtubules
Receptors & Channels	Channels	amiodarone	10.0uM-41.1nM,0nM	NA Channels
	GPCRs	bendroflumethiazide	1.0uM-2.6nM,0nM	Cl channel
		cabozantinib	4.0uM-0.1nM,0nM	C-Met/Axl/Ret
		dronedarone	10.0uM-41.1nM,0nM	NA Channels
		ivacaftor	10.0uM-41.1nM,0nM	CFTR
		nateglinide	1.0uM-2.6nM,0nM	ATP-dependent K channels
		acetylcysteine	10.0uM-41.1nM,0nM	Glutamate receptor
		aprepitant	10.0uM-41.1nM,0nM	Neuromedin receptor
		beclomethasone dipropionate	1.0uM-2.6nM,0nM	Glucocorticoid receptor
		loratadine	10.0uM-41.1nM,0nM	Histamine H1-receptors
		naftopidil	10.0uM-41.1nM,0nM	B1-adrenergic receptor
	MAPK-RTKIs	nebivolol	10.0uM-41.1nM,0nM	B1 receptor
		sp600125	10.0uM-41.1nM,0nM	JNK
		thioridazine	10.0uM-41.1nM,0nM	Adrenergic receptor
		afatinib	4.0uM-0.1nM,0nM	EGFR/HER2
		ag 879	1.0uM-2.6nM,0nM	HER2/RAF-1
		gefitinib	4.0uM-0.1nM,0nM	EGFR
		gsk1751853a	10.0uM-41.1nM,0nM	IGF1R/INSR
		gsk994854a	10.0uM-41.1nM,0nM	IGF1R/INSR
		gw458787a	10.0uM-41.1nM,0nM	EGFR/ERBB4
		gw644007x	10.0uM-41.1nM,0nM	Ret
		gw694590a	10.0uM-41.1nM,0nM	TIE2
		gw770249x	10.0uM-41.1nM,0nM	FLT3
		linsitinib	5.0uM-19.5nM,0nM	IGF1R
		ponatinib	4.0uM-0.1nM,0nM	FGFR
		tyrphostinag370	10.0uM-41.1nM,0nM	PDGFRbeta
BRAF- Mutant Melanoma	MAPK/PI3K	dabrafenib	0.4nM-0.39nM,0nM	BRAFV600
		plx4720	8.0uM-7.8nM,0nM	BRAFV600E & CRAF1
		raf265	1.0uM-3.9nM,0nM	CRAF,BRAF, &
		vemurafenib	8.0uM-7.8nM,0nM	BRAFV600E BRAFV600
Kinases	MAPK/PI3K			

	selumetinib	4.0uM-61pM,0nM	MEK1
	trametinib	0.4uM-6.1pM,0nM	MEK1/2
	pd98059	0.4uM-6.1pM,0nM	MEK1
	cobimetinib	0.8uM-12pM,0nM	MEK1

Table S3: BRAFi sensitivity across CCLE BRAF-mutant melanoma cell line panel. Related to Figure 3.

CCLE Cell Line	DIP Rate (h^{-1}) at [8uM] PLX4270
<i>A2058_SKIN</i>	0.030
<i>A375_SKIN</i>	0.005
<i>SKMEL28_SKIN</i>	0.010
<i>SKMEL5_SKIN</i>	0.014
<i>WM115_SKIN</i>	0.013
<i>WM1799_SKIN</i>	-0.002
<i>WM2664_SKIN</i>	0.003
<i>WM793_SKIN</i>	0.015
<i>WM88_SKIN</i>	-0.020
<i>WM983B_SKIN</i>	0.021

Table S4: Differentially Expressed Genes (DEGs) between SKMEL5 subclones SC01, SC07, SC10 whose expression significantly correlated to BRAFi insensitivity (Pearson r) across panel of 10 cell-lines (expression data from (Subramanian et al., 2017)). See Table S3 for quantification of sensitivity to BRAFi. Related to Figure 3.

Positive Correlation with BRAFi insensitivity			Negative Correlation with BRAFi insensitivity		
Gene symbol	r	p-value	Gene symbol	r	p-value
SLC7A11	0.816	0.004	GRIK3	-0.743	0.014
SLC16A7	0.807	0.005	PRELP	-0.720	0.019
TGFB1	0.666	0.036	CPVL	-0.684	0.029
NOX5	0.649	0.042	ITGA10	-0.659	0.038
LXN	0.646	0.044			

Table S5: Description of nested model tiers used in MCMC fit. Related to STAR Methods.

Model Tier	Fit Parameters	Approximations
#5	$\alpha_1, \alpha_2, E_3, E_1, E_2, C_1, C_2, h1, h2, E_0, r_1, r_2$	1. Rate of transition (r1,r2) $\gg 1$.
#4	$\alpha_2, E_3, E_1, E_2, C_1, C_2, h1, h2, E_0$	1. System obeys detail balance.
#3	$\alpha_2, E_3, E_1, E_2, C_1, C_2, h1, h2$	1. All conditions tier 4 2. E0 is the minimally observed effect.
#2	$\alpha_2, E_3, E_1, E_2, C_1, C_2$	1. All conditions tiers 3,4 2. h1,h2 are from single drug fits or 1 if single fits failed to converge.
#1	α_2, E_3, E_1, E_2	1. All conditions tiers 2-4 2. C1,C2 are from single drug fits or the median concentration if single fits failed to converge.
#0	α_2, E_3	1. All conditions tiers 1-4 2. E1, E2 are assumed to be the maximally observed effect at maximum concentration of d1 and d2 respectively.

2 Supplemental Text

2.1 Key equations

For full derivation of these equations, see section titled Derivation of 2D Hill Equation. This section is meant to serve as a quick reference guide for the main equations used in the paper.

If the behavior of the drugs in the model formulation of Figure S1 obey detailed balance, then the averaged effect (height of combination surface) is described by

$$E_d = \frac{C_1^{h_1} C_2^{h_2} E_0 + d_1^{h_1} C_2^{h_2} E_1 + C_1^{h_1} d_2^{h_2} E_2 + (\alpha_2 d_1)^{h_1} d_2^{h_2} E_3}{C_1^{h_1} C_2^{h_2} + d_1^{h_1} C_2^{h_2} + C_1^{h_1} d_2^{h_2} + (\alpha_2 d_1)^{h_1} d_2^{h_2}} \quad (1)$$

where E_d represents the expected effect for a given dose pair d_1, d_2 and is specified with 9 dose response parameters defined in Table S1. In addition, detailed balance enforces the constraint that

$$\alpha_1^{h_2} = \alpha_2^{h_1} \quad (2)$$

α is a unitless scalar transforming dose d into an effective dose $\alpha \cdot d$, and is used to quantify synergistic potency in MuSyC.

Synergistic efficacy (β) is found from E_0, E_1, E_2, E_3 . β is defined in equation 3 and is interpreted as the percent increase in efficacy of the combination over the most efficacious single agent. The observed β at the maximum of tested concentrations is defined in eq. 4.

$$\beta = \frac{\min(E_1, E_2) - E_3}{E_0 - \min(E_1, E_2)} \quad (3)$$

$$\beta_{obs} = \frac{\min[E_1(d1_{max}), E_2(d2_{max})] - E_3(d1_{max}, d2_{max})}{E_0 - \min[E_1(d1_{max}), E_2(d2_{max})]} \quad (4)$$

The equation 1 can be re-written to include β by replacing E_3 with $\min(E_1, E_2) - \beta * (E_0 - \min(E_1, E_2))$ resulting in the following equation.

$$E_d = \frac{C_1^{h_1} C_2^{h_2} E_0 + d_1^{h_1} C_2^{h_2} E_1 + C_1^{h_1} d_2^{h_2} E_2 + (\alpha_2 d_1)^{h_1} d_2^{h_2} (\min(E_1, E_2) - \beta * (E_0 - \min(E_1, E_2)))}{C_1^{h_1} C_2^{h_2} + d_1^{h_1} C_2^{h_2} + C_1^{h_1} d_2^{h_2} + (\alpha_2 d_1)^{h_1} d_2^{h_2}} \quad (5)$$

For drugs that do not follow detailed balance, we have derived a more general formulation with 12 parameters:

$$E_d = [E_0 \quad E_1 \quad E_2 \quad E_3] \cdot \begin{bmatrix} - (r_1 d_1^{h_1} + r_2 d_2^{h_2}) & r_{-1} & r_{-2} & 0 \\ r_1 d_1^{h_1} & - (r_{-1} + r_2 (\alpha_1 d_2)^{h_2}) & 0 & r_{-2} \\ r_2 d_2^{h_2} & 0 & - (r_1 (\alpha_2 d_1)^{h_1} + r_{-2}) & r_{-1} \\ 1 & 1 & 1 & 1 \end{bmatrix}^{-1} \cdot \begin{bmatrix} 0 \\ 0 \\ 0 \\ 1 \end{bmatrix} \quad (6)$$

where again E_3 can be replaced to include β .

Because we do not know *a priori* whether combinations will follow detailed balance, we use an information theoretic approach to pick the best model for the data. We have defined six tiers of model complexity, and the best model is selected based on minimizing the deviance information criterion. (See methods for fitting dose-response surfaces and Table S5 for description of model tiers).

2.2 Comparison to alternative synergy models

Several other methods for calculating synergy exist, including long-standing traditional methods Loewe (Loewe, 1927), Bliss (BLISS, 1939), HSA Greco et al. (1995), and CI (Chou and Talalay, 1984), as well as more recent methods such as ZIP (Yadav et al., 2015), BRAID (Twarog et al., 2016), the effective dose model (Zimmer et al., 2016), and Schindler’s recent Hill-PDE model (Schindler, 2017). All of these methods, as well as our own, define a null surface. Combinations with effects greater than or less than expected per the null surface are deemed synergistic or antagonistic respectively. These methods broadly use one of two approaches to quantify synergy. Loewe, Bliss, CI, HSA, Schindler’s Hill-PDE, and ZIP quantify synergy at every concentration based on how the experimentally measured response relates to the null surface. Conversely, BRAID, the effective dose model, and MuSyC provide equations describing the entire surface, containing synergy parameters which are fit to experimental data using non-linear curve-fitting techniques.

Here, we briefly compare our model to each of these others and show that our model (1) describes distinct combination surfaces, (2) results in synergy parameters which are straight forward to interpret, (3) is not restricted to a special class of effects with bounded scales, and (4) reduces to many of these other approaches in special cases thereby unifying and generalizing seemingly disparate synergy principles.

2.2.1 The Dose Equivalence Principle: Loewe and CI

The first prevalent foundational principle, established by Loewe (Loewe, 1926), and subsequently expanded on by CI (Chou and Talalay, 1984), is the dose equivalence principle. This states that for a given effect magnitude E , such that dose x of drug X alone, or dose y of drug Y alone achieves that effect, then there is a constant ratio $R = \frac{x}{y}$ such that using a less of drug X can always be compensated for by using $b = Ra$ more of drug Y. Therefore, the null surface is only defined for combinations

whose magnitude of effect is less than the *weaker* drug’s maximal effect. This is because beyond such concentrations, no amount y of the weaker drug can compensate for reducing the dose of the stronger drug by x .

The resulting null surfaces have linear isoboles. Our model recovers this under the constraint that the two drugs are maximally antagonistic. This can be seen by setting $\alpha = 0$, and reducing eq. 44 to

$$(E - E_0) + (E - E_1) \left(\frac{d_1}{\Phi_1} \right)^{h_1} + (E - E_2) \left(\frac{d_2}{\Phi_2} \right)^{h_2} = 0$$

By this it is easy to see when $h_1 = h_2 = 1$, iso-effect lines are represented by the linear isoboles characteristic of Loewe Additivity and the CI null models. However, even in this case MuSyC is not limited by the weaker drug, and can therefore extend Loewe’s isoboles to any combination doses.

The requirement that $\alpha = 0$ means the Loewe and CI null models assumes infinite potency antagonism ($\alpha_1 = \alpha_2 = 0$). Therefore, combinations with ($0 < \alpha < 1$) may be deemed synergistic by Loewe or CI. However, these values directly reflect a decrease in potency, and our formulation accurately identifies this as antagonistic. Finally, their null model also ignores the possible effect of hill slopes not equal to 1. For drugs with $h < 1$, they will tend to overestimate synergy, while drugs with $h > 1$ will lead to underestimated synergy (see Figure 4C,D). Because their null model relies on such specific assumptions, which are not true for many drugs, it is generally impossible to know whether their results reflect true underlying synergy/antagonism, or simply stem from an inappropriate null surface.

2.2.2 The Multiplicative Survival Principle: Bliss and Effective Dose Model

The other prevalent foundational synergy principle is multiplicative survival, described by Bliss (BLISS, 1939). Bliss defines a null model by assuming the probability of a cell being unaffected by drug 1 (U_1) is independent of the probability of a cell being unaffected by drug 2 (U_2). From this, the null surface states the probability of being unaffected by both drug 1 and drug 2 in combination is $U_{1,2} = U_1 \cdot U_2$ (BLISS, 1939). When there is no potency synergy or antagonism, MuSyC reproduces this behavior in the following manner.

Setting $\alpha_1 = \alpha_2 = 1$, consider the fraction of unaffected cells, U , for each drug in isolation:

$$U_i = \frac{1}{1 + \left(\frac{d_i}{\Phi_i} \right)^{h_i}}$$

And for the two drugs in combination we get

$$U_{1,2} = \frac{1}{1 + \left(\frac{d_1}{\Phi_1} \right)^{h_1} + \left(\frac{d_2}{\Phi_2} \right)^{h_2} + \left(\frac{d_1}{\Phi_1} \right)^{h_1} \left(\frac{d_2}{\Phi_2} \right)^{h_2}}$$

From this, it is easy to verify that $U_{1,2} = U_1 \cdot U_2$, which is equivalent to Bliss Independence. However, the Bliss method explicitly requires the effect being measured in the combination surface is "percent affected", such as percent of cells killed vs. percent of cells remaining. For drugs which induce different maximum effects, Bliss is unable to account for the difference between being affected by drug 1 (E_1), drug 2 (E_2), and or both ($E_{1,2}$), and may give unreliable results if the two drugs do not have identical maximum effect. Our model addresses this by decoupling the effect of a drug (E_0, E_1, E_2, E_3) and the "percent affected" by a drug ($U, A_1, A_2, A_{1,2}$). If the effect itself is measuring percent (un)affected, that corresponds to the case where $E_0 = 1, E_1 = E_2 = E_3 = 0$, in which case MuSyC’s null model is identical to Bliss’.

Zimmer et. al. introduced the effective dose model (Zimmer et al., 2016) as an extension of Bliss, and shares the same null surface. However, while Bliss defines synergy at every concentration independently, the effective dose model introduces a parameter $a_{i,j}$, similar to our potency synergy (α) in our formulation. The $a_{i,j}$ parameter reflects how the presence of drug i modulates the potency of drug j . However, like Bliss, the effective dose model can still only be applied to drug responses where the measured drug effect is "percent affected". Furthermore, their formulation requires the maximum effect of both drugs is 100% affected which is commonly not observed (Fallahi-Sichani et al., 2013).

2.2.3 ZIP

Like the Equivalent Dose Model (Zimmer et al., 2016), as well as our potency synergy (α), ZIP works by quantifying how one drug shifts the potency of the other. ZIP is formulated for arbitrary E_0 and E_{max} ; however, it assumes E_{max} is the same for both drugs, as well as the combination (explicitly $E_1 = E_2 = E_3$). To identify potency shifts, the ZIP method fixes the concentration of one drug, then fits a Hill-equation dose response for the other drug. However, for combinations with efficacy synergy or antagonism, dose responses can have non-Hill, and even non-monotonic shapes. In our data, several drugs displayed this behavior. Because our method accounts explicitly for efficacy synergy, our surfaces are able to describe such complex drug combination surfaces where ZIP fails.

Furthermore, ZIP calculates synergy at every concentration. This is similar to the approach taken by Bliss, Loewe, and CI, and can be used to find doses which maximize the observed synergy. Nevertheless, quantifying synergy on a dose-by-dose basis confounds synergy of potency and efficacy which emerge as only on inspection of the global dose-response surface. Additionally, this dose dependence often leads to ambiguous results about whether a given combination is synergistic or not, as it synergizes at some concentrations, and antagonizes at others (Figure 4A).

2.2.4 BRAID

Like ZIP, BRAID assumes that each drug alone has a sigmoidal dose-response, and constructs a Hill-like equation for the combination. This equation uses a single dose parameter which combines the doses of both individual drugs using a parameter κ . To uniquely solve for κ , this formalism, like Loewe additivity, adds the constraint that a drug in combination with itself must be neither synergistic nor antagonistic. By adjusting κ , BRAID is able to fit complex drug combination surfaces, including non-monotonic responses. Because BRAID fits the whole combination surface using a single parameter, it can be used to make unambiguous statements about whether the combination is synergistic or antagonistic. Nevertheless, BRAID does not account for differences in synergy due to efficacy vs. potency, whereas we find many combinations that are synergistic with respect to one, but antagonistic with respect to the other. Indeed, the biochemical interpretation of κ is not straightforward. Furthermore, the BRAID model is unable to fit combination surfaces with synergistic efficacy, as it assumes that the maximum effect of the combination is equal to the maximum effect of the stronger single-drug mirroring the limitation of Loewe Additivity.

2.2.5 Highest Single Agent (HSA)

HSA, originally proposed by Gaddum in 1940 and then revived later by Greco (Greco et al., 1995), is a simple heuristic which argues synergy is any combination effect which exceeds the efficacy of either single agent. While β is conceptually similar to HSA, β provides a global view of the possible increase in effect rather than a point by point dose comparison as done in HSA. Because HSA is calculated at every dose it cannot distinguish between synergistically efficacious combinations and synergistically potent combinations as both will result increase the effect at intermediate doses (Figure S3). Additionally, as HSA is only defined on a dose by dose basis with no model fit, it is sensitive to the dose range selected and cannot estimate uncertainty in synergy for different dose intervals as MuSyC does.

2.2.6 Schindler 2D-Partial Differential Equation (PDE) Model

Schindler’s Hill PDE was derived to impute the dose response surface from the single dose response curves alone (Schindler, 2017). Therefore, it does not contain any parameters fit synergy but rather defines a null surface for which synergy results in deviations in the surface. While Schindler did not specify how to account for these deviations, he postulates some implementation of perturbation theory would be sufficient. Like CI and the Equivalent Dose Model, Schindler’s framework requires effects in a range between 0 and 1, based on the assumption that the metric is a percent. Therefore, Schindler cannot be applied to data collected with other types of metrics (e.g. DIP Rates). Additionally, Schindler’s because the maximum effect of the combination is set equal to the average of the single drug

maximal effect (to allow for smooth transitions between the two single dose-response curves), some non-intuitive solutions arise. For example, if drug 1 has a maximal effect of 50% and drug 2 has a maximal effect of 70% the expected maximal effect of the combination in the null model is 60% which is less than the maximal effect of drug 1. Therefore, an effect of 65% in combination, though less than achievable with one drug, is designated synergistic by Schindler.

2.3 Sham Experiment

It is common for synergy metrics to examine the special case in which the two drugs being combined are actually the same drug. Because our method distinguishes between two types of synergy, we tested sham compliance for each independently. It is immediately apparent synergistic efficacy is sham complaint in all conditions. This can be observed by substituting $E_1 = E_2 = E_3$, indicating the maximum effect of the drug remains the same into the definition for β in equation 3

$$\beta = \frac{\min(E_1, E_2) - E_3}{E_0 - \min(E_1, E_2)} = 0 \quad (7)$$

To test the sham compliance of synergistic potency, we can write the full dose response surface as a direct 2D extension of the 1D dose response curve in equation 12 by replacing d with $d_1 + d_2$.

$$E_d = \frac{E_m(d_1 + d_2)^h + E_0C^h}{(d_1 + d_2)^h + C^h} \quad (8)$$

Our 2D generalization of equation 12, given by equation 44 can be rewritten for the case of 2 identical drugs by observing that $C_1 = C_2 = C$, $h_1 = h_2 = h$, and $E_1 = E_2 = E_3 = E_m$, resulting in

$$E_d = \frac{C^{2h}E_0 + d_1^hC^hE_m + C^hd_2^hE_m + (\alpha_2d_1d_2)^hE_m}{C^{2h} + d_1^hC^h + C^hd_2^h + (\alpha_2d_1d_2)^h}. \quad (9)$$

Setting equations 8 and 9 equal to one another, we find

$$\alpha_2 = C^h \frac{(d_1 + d_2)^h - d_1^h - d_2^h}{(d_1d_2)^h}, \quad (10)$$

This equation is valid when $\alpha_2 = \alpha_1 = 0$ and $h = 1$. This makes sense as our model reduces to Loewe additivity under those conditions, and Loewe additivity was developed to explicitly address the sham-combination case. In conclusion, MuSyC satisfies the sham experiment in all conditions where Loewe is the appropriate model.

3 Derivation of generalized 2-dimensional hill equation

3.1 One-dimensional sigmoidal dose-response curve

In pharmacology, the effect of a drug is usually described by the Hill equation, which arises from the equilibrium of a reversible transformation between an unaffected population (U) and an affected population (A)

$$U + h \cdot d \xrightleftharpoons[r_{-1}]{r_1} A \quad (11)$$

Here, d is the concentration of the drug, h is the Hill slope, and r_1 and r_{-1} are constants corresponding to its rate of action. Solving for the equilibrium results in

$$\begin{aligned} \frac{dU}{dt} &= A \cdot r_{-1} - U \cdot r_1 d^h \equiv 0 \\ \frac{A}{U} &= \frac{r_1 d^h}{r_{-1}} \end{aligned}$$

When $d^h = \frac{r_{-1}}{r_1}$, then half the population is affected, and half is unaffected ($A = U$). This dose is the EC50, denoted as $C^h = \frac{r_{-1}}{r_1}$. Adding the constraint that $U + A = 1$, which states that 100% of the population is either unaffected or affected, we find the classic Hill equation:

$$U = \frac{C^h}{C^h + d^h}$$

If the unaffected and affected populations differ phenotypically by some arbitrary effect (such as proliferation rate), the average observed effect over the whole population at dose d of some drug will be a weighted average of the two effects by the percent affected and unaffected. Namely,

$$E_d = U \cdot E_0 + A \cdot E_m,$$

where E_0 is the effect characteristic of the unaffected population, and E_m is the effect characteristic of the affected population. From this we find the final form of a 4-parameter sigmoidal equation describing dose-response due to Hill-kinetics:

$$\frac{E_d - E_m}{E_0 - E_m} = \frac{C^h}{C^h + d^h} \quad (12)$$

3.2 Extending the mass action paradigm to simple four-state model assuming detailed balance

Consider a cell type U that can transition into a “drugged” state A_1 in the presence of drug d_1 and into a different drugged state A_2 in the presence of drug d_2 (Figure S1A). We can write these transitions as



where $[d_i]$ denotes concentration of drug d_i . At equilibrium, the forward and reverse rates of these processes are equal, i.e.,

$$r_1[d_1][U] = r_{-1}[A_1], \quad (15)$$

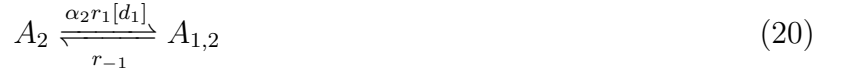
$$r_2[d_2][U] = r_{-2}[A_2], \quad (16)$$

where $[A_i]$ is the population of cell state A_i . Defining Θ_x as the ratio of forward and reverse rates ($\Theta_x \equiv r_{-x}/r_x$) and assuming the system obeys detail balance, we find

$$\frac{[U]}{[A_1]} = \frac{\Theta_1}{[d_1]}, \quad (17)$$

$$\frac{[U]}{[A_2]} = \frac{\Theta_2}{[d_2]}, \quad (18)$$

Now assume that a fourth state exists, $A_{1,2}$, corresponding to a “doubly” drugged state (Figure S1B). A_1 cells can transition into this state in the presence of drug d_2 and A_2 cells can transition into this state in the presence of drug d_1 . We can write these processes as



Note that without loss of generality, we set the forward rate constant for (19) equal to the same value in (14) multiplied by a factor $\alpha_1 > 0$. Similarly, the rate constant for (20) is the same as in (13) multiplied by a factor $\alpha_2 > 0$. Here α represents how each drug potentiates the action of the other and can be interpreted as a change in the “effective” dose of one drug given the presence of the other.

Again asserting the system obeys detailed balance at equilibrium, we have

$$\frac{[A_1]}{[A_{1,2}]} = \frac{1}{\alpha_1} \frac{\Theta_2}{[d_2]}, \quad (21)$$

$$\frac{[A_2]}{[A_{1,2}]} = \frac{1}{\alpha_2} \frac{\Theta_1}{[d_1]}. \quad (22)$$

We can derive the relationship between the multiplicative factors α_1 and α_2 by rearranging Eq. (17) as

$$[U] = \frac{\Theta_1}{[d_1]} [A_1]. \quad (23)$$

Substituting for $[A_1]$ from Eq. (21) gives

$$[U] = \frac{1}{\alpha_1} \frac{\Theta_1}{[d_1]} \frac{\Theta_2}{[d_2]} [A_{1,2}]. \quad (24)$$

Substituting for $[A_{1,2}]$ from Eq. (22) gives

$$[U] = \frac{\alpha_2}{\alpha_1} \frac{\Theta_2}{[d_2]} [A_2]. \quad (25)$$

Finally, substituting for $[A_2]$ from Eq. (18) gives

$$[U] = \frac{\alpha_2}{\alpha_1} [U], \quad (26)$$

i.e., $\alpha_1 = \alpha_2 = \alpha$. Note this equality only holds for systems obeying detailed balance. In general, we do not assume this (See Section ‘Generalized derivation without assuming detailed balance’) and $\alpha_1 = \alpha_2$ are independent (Figure S4).

Now, we define the total cell count

$$C_T \equiv [U] + [A_1] + [A_2] + [A_{1,2}]. \quad (27)$$

Substituting for $[A_1]$, $[A_2]$, and $[A_{1,2}]$ from Eqs. (17), (18), and (24), respectively, gives

$$C_T = [U] + \frac{[d_1]}{\Theta_1} [U] + \frac{[d_2]}{\Theta_2} [U] + \alpha \frac{[d_1]}{\Theta_1} \frac{[d_2]}{\Theta_2} [U]. \quad (28)$$

Solving for $[U]$ gives

$$[U] = \frac{\Theta_1 \Theta_2 C_T}{\Theta_1 \Theta_2 + [d_1] \Theta_2 + \Theta_1 [d_2] + \alpha [d_1] [d_2]}. \quad (29)$$

Substituting Eq. (29) into Eq. (17) and rearranging gives

$$[A_1] = \frac{[d_1] \Theta_2 C_T}{\Theta_1 \Theta_2 + [d_1] \Theta_2 + \Theta_1 [d_2] + \alpha [d_1] [d_2]}. \quad (30)$$

Similarly, from Eq. (18) we get

$$[A_2] = \frac{\Theta_1 [d_2] C_T}{\Theta_1 \Theta_2 + [d_1] \Theta_2 + \Theta_1 [d_2] + \alpha [d_1] [d_2]}, \quad (31)$$

and from Eq. (24)

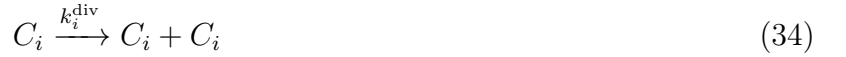
$$[A_{1,2}] = \frac{\alpha [d_1] [d_2] C_T}{\Theta_1 \Theta_2 + [d_1] \Theta_2 + \Theta_1 [d_2] + \alpha [d_1] [d_2]}. \quad (32)$$

The measured effect (E_d) is then the relative proportion of cells in each state multiplied by the effect characteristic of that state as in

$$E_d = E_0 * U + E_1 * A_1 + E_2 * A_2 + E_3 * A_{1,2} \quad (33)$$

Here we define the effect of each state to be proliferation rate in the following way.

We assume that cells in each state can divide and die at rates characteristic of the state, i.e.,



where C_i is specific state of the cell.

We define the drug-induced proliferation (DIP) rate for each state as the difference between the division and death rate constants, i.e.,

$$k_i^{\text{dip}} \equiv k_i^{\text{div}} - k_i^{\text{die}}. \quad (36)$$

Using Eq. (27), the rate of change of the total cell population is

$$\frac{dC_T}{dt} = \frac{d[U]}{dt} + \frac{d[A_1]}{dt} + \frac{d[A_2]}{dt} + \frac{d[A_{1,2}]}{dt}. \quad (37)$$

From (13), (14), (19), (20), (34)–(36), we get

$$\frac{dC_T}{dt} = k_0^{\text{dip}} [U] + k_1^{\text{dip}} [A_1] + k_2^{\text{dip}} [A_2] + k_3^{\text{dip}} [A_{1,2}]. \quad (38)$$

Substituting Eqs. (29)–(32) and rearranging, we get

$$\frac{dC_T}{dt} = k_T^{\text{dip}} C_T \quad (39)$$

with

$$k_T^{\text{dip}} \equiv \frac{\Theta_1 \Theta_2 k_0^{\text{dip}} + [d_1] \Theta_2 k_1^{\text{dip}} + \Theta_1 [d_2] k_2^{\text{dip}} + \alpha [d_1] [d_2] k_3^{\text{dip}}}{\Theta_1 \Theta_2 + [d_1] \Theta_2 + \Theta_1 [d_2] + \alpha [d_1] [d_2]}. \quad (40)$$

Note that with a slight modification, Eq. (40) can be written as

$$k_T^{\text{dip}} = \frac{\Theta_1 k_0^{\text{dip}} + [d_1] k_1^{\text{dip}} + \frac{\Theta_1 [d_2]}{\Theta_2} k_2^{\text{dip}} + \frac{\alpha [d_1] [d_2]}{\Theta_2} k_3^{\text{dip}}}{\Theta_1 + [d_1] + \frac{\Theta_1 [d_2]}{\Theta_2} + \frac{\alpha [d_1] [d_2]}{\Theta_2}}. \quad (41)$$

Therefore, if $[d_2] = 0$ (i.e., single-drug treatment) we get

$$\begin{aligned}
k_T^{\text{dip}} &= \frac{\Theta_1 k_0^{\text{dip}} + [d_1] k_1^{\text{dip}}}{\Theta_1 + [d_1]} \\
&= \frac{\Theta_1 k_0^{\text{dip}} + [d_1] k_1^{\text{dip}} + (\Theta_1 k_1^{\text{dip}} - \Theta_1 k_1^{\text{dip}})}{\Theta_1 + [d_1]} \\
&= \frac{(\Theta_1 + [d_1]) k_1^{\text{dip}} + \Theta_1 (k_0^{\text{dip}} - k_1^{\text{dip}})}{\Theta_1 + [d_1]} \\
&= k_1^{\text{dip}} + \frac{\Theta_1}{\Theta_1 + [d_1]} (k_0^{\text{dip}} - k_1^{\text{dip}}).
\end{aligned} \tag{42}$$

Rearranging gives

$$\frac{k_T^{\text{dip}} - k_1^{\text{dip}}}{k_0^{\text{dip}} - k_1^{\text{dip}}} = \frac{\Theta_1}{\Theta_1 + [d_1]}. \tag{43}$$

Comparing to Eq. (12), we see that Eq. (43) is a one-dimensional sigmoidal dose-response curve with $E_d = k_T^{\text{dip}}$, $E_0 = k_0^{\text{dip}}$, $E_m = k_1^{\text{dip}}$, $C = \Theta_1$, and $h = 1$. By analogy, we surmise that Eq. (40) is a nine parameter, two-dimensional generalization of Eq. (12), i.e.,

$$E_d = \frac{C_1^{h_1} C_2^{h_2} E_0 + d_1^{h_1} C_2^{h_2} E_1 + C_1^{h_1} d_2^{h_2} E_2 + (\alpha_2 d_1)^{h_1} d_2^{h_2} E_3}{C_1^{h_1} C_2^{h_2} + d_1^{h_1} C_2^{h_2} + C_1^{h_1} d_2^{h_2} + (\alpha_2 d_1)^{h_1} d_2^{h_2}}, \tag{44}$$

with $E_d = k_T^{\text{dip}}$, $E_0 = k_0^{\text{dip}}$, $E_1 = k_1^{\text{dip}}$, $E_2 = k_2^{\text{dip}}$, $E_3 = k_3^{\text{dip}}$, $C_1 = \Theta_1$, $C_2 = \Theta_2$, $h_1 = 1$, $h_2 = 1$, and the additional parameter α_2 . Note that under the assumption of detailed balance we found $\alpha_1 = \alpha_2$ for the case when $h = 1$. Therefore, in the general case when $h \neq 1$, $\alpha_1^{h_2} = \alpha_2^{h_1}$. By fitting the equation 44, α_1 is uniquely determined.

3.3 Four-state model with multiple steps between states

Let us assume that instead of occurring in a single step, the cell state transitions are h step processes, i.e.,

$$C_i \xrightleftharpoons[r_{-x,1}]{r_{x,1}[\alpha_x d_x]} C_{ij}^1 \xrightleftharpoons[r_{-x,2}]{r_{x,2}[\alpha_x d_x]} C_{ij}^2 \cdots \xrightleftharpoons[r_{-x,h-1}]{r_{x,h-1}[\alpha_x d_x]} C_{ij}^{h-1} \xrightleftharpoons[r_{-x,h}]{r_{x,h}[\alpha_x d_x]} C_j \tag{45}$$

Assuming that all steps are in rapid equilibrium, it is straightforward to show that

$$\frac{[C_i]}{[C_j]} = \frac{\prod_{m=1}^h \Theta_{x,m}}{[\alpha_x d_x]^h}, \tag{46}$$

where $\Theta_{x,m} \equiv r_{-x,m}/r_{x,m}$. Defining $\Phi_x \equiv \sqrt[h]{\prod_{m=1}^h \Theta_{x,m}}$, Eq. (46) can be written as

$$\frac{[C_i]}{[C_j]} = \frac{\Phi_x^h}{[\alpha_x d_x]^h} \tag{47}$$

which is the well-known Median-Effect Equation from Chou (Chou et al., 1983; Chou, 2010; Chou and Talalay, 1984). Replacing reactions (13) and (14) with multi-step processes of the form (45), gives us

$$\frac{[U]}{[A_1]} = \frac{\Phi_1^{h_1}}{[d_1]^{h_1}}, \tag{48}$$

$$\frac{[U]}{[A_2]} = \frac{\Phi_2^{h_2}}{[d_2]^{h_2}}. \tag{49}$$

Similarly, we replace reactions (19) and (20) with the same multi-step process except with the rate constant for the $C_i \rightarrow C_i^1$ transition (entry into the cascade) equal to $\alpha_x r_{x,1}[d_x]$, giving

$$\frac{[A_1]}{[A_{1,2}]} = \frac{\Phi_2^{h_2}}{[\alpha_1 d_2]^{h_2}}, \quad (50)$$

$$\frac{[A_2]}{[A_{1,2}]} = \frac{\Phi_1^{h_1}}{[\alpha_2 d_1]^{h_1}}. \quad (51)$$

Note that we assume that the number of steps in the cascade (45) is dependent on the drug type (i.e., $U \rightarrow A_1$ and $A_2 \rightarrow A_{1,2}$, both driven by d_1 , take h_1 steps, while $U \rightarrow A_2$ and $A_1 \rightarrow A_{1,2}$, both driven by d_2 , take h_2 steps). Using Eqs. (48)–(51) and again defining the total cell count C_T as in Eq. (27), we derive

$$[U] = \frac{\Phi_1^{h_1} \Phi_2^{h_2} C_T}{\Phi_1^{h_1} \Phi_2^{h_2} + [d_1]^{h_1} \Phi_2^{h_2} + \Phi_1^{h_1} [d_2]^{h_2} + [\alpha_2 d_1]^{h_1} [d_2]^{h_2}}, \quad (52)$$

$$[A_1] = \frac{[d_1]^{h_1} \Phi_2^{h_2} C_T}{\Phi_1^{h_1} \Phi_2^{h_2} + [d_1]^{h_1} \Phi_2^{h_2} + \Phi_1^{h_1} [d_2]^{h_2} + [\alpha_2 d_1]^{h_1} [d_2]^{h_2}}, \quad (53)$$

$$[A_2] = \frac{\Phi_1^{h_1} [d_2]^{h_2} C_T}{\Phi_1^{h_1} \Phi_2^{h_2} + [d_1]^{h_1} \Phi_2^{h_2} + \Phi_1^{h_1} [d_2]^{h_2} + [\alpha_2 d_1]^{h_1} [d_2]^{h_2}}, \quad (54)$$

$$[A_{1,2}] = \frac{\alpha [d_1]^{h_1} [d_2]^{h_2} C_T}{\Phi_1^{h_1} \Phi_2^{h_2} + [d_1]^{h_1} \Phi_2^{h_2} + \Phi_1^{h_1} [d_2]^{h_2} + [\alpha_2 d_1]^{h_1} [d_2]^{h_2}}. \quad (55)$$

Therefore, in the same way that we arrived at Eq. (40), we can derive

$$k_T^{\text{dip}} \equiv \frac{\Phi_1^{h_1} \Phi_2^{h_2} k_0^{\text{dip}} + [d_1]^{h_1} \Phi_2^{h_2} k_1^{\text{dip}} + \Phi_1^{h_1} [d_2]^{h_2} k_2^{\text{dip}} + [\alpha_2 d_1]^{h_1} [d_2]^{h_2} k_3^{\text{dip}}}{\Phi_1^{h_1} \Phi_2^{h_2} + [d_1]^{h_1} \Phi_2^{h_2} + \Phi_1^{h_1} [d_2]^{h_2} + [\alpha_2 d_1]^{h_1} [d_2]^{h_2}}, \quad (56)$$

which is of the form Eq. (44) with $E_d = k_T^{\text{dip}}$, $E_0 = k_0^{\text{dip}}$, $E_1 = k_1^{\text{dip}}$, $E_2 = k_2^{\text{dip}}$, $E_3 = k_3^{\text{dip}}$, $C_1 = \Phi_1$, and $C_2 = \Phi_2$. From this it is clear the hill coefficient (h) is related to the number of intermediate steps in the system.

The derivation of Eq. (56) assumes that the populations of all intermediate cell states C_{ij}^m ($m \in \{1 \dots h-1\}$) in (45) are small (≈ 0).¹ We can satisfy this assumption by requiring that all $r_{x,m}$, $r_{-x,m} \gg 1$ ($m \in \{1 \dots h\}$) and $\Theta_{x,1} \gg \Theta_{x,2} \approx \dots \approx \Theta_{x,h-1} \gg \Theta_{x,h}$. To see this, consider cell state U and all of its intermediate states between states A_1 and A_2 . Let us define

$$U^T \equiv [U] + \sum_{m=1}^{h_1-1} [C_{01}^m] + \sum_{m'=1}^{h_2-1} [C_{02}^{m'}]. \quad (57)$$

From (45), we see that $\Theta_{x,1}/[d_x] = [C_i]/[C_{ij}^1]$, $\Theta_{x,2}/[d_x] = [C_{ij}^1]/[C_{ij}^2]$, etc. Therefore,

$$U^T = [U] \left(1 + \frac{[d_1]}{\Theta_{1,1}} + \frac{[d_1]^2}{\Theta_{1,1}\Theta_{1,2}} + \dots + \frac{[d_1]^{h_1-1}}{\prod_{m=1}^{h_1-1} \Theta_{1,m}} + \frac{[d_2]}{\Theta_{2,1}} + \frac{[d_2]^2}{\Theta_{2,1}\Theta_{2,2}} + \dots + \frac{[d_2]^{h_2-1}}{\prod_{m'=1}^{h_2-1} \Theta_{2,m'}} \right). \quad (58)$$

¹This is most evident in our use of Eq. (27) for the total cell population, where we only consider the end states. However, it is also implicit in our use of Eq. (46), which is used to derive Eqs. (52)–(55) that lead to Eq. (56) via Eq. (38). In other words, we are assuming that the intermediate states do not significantly contribute to the dynamics of the total cell population. Since it is not reasonable to assume that cells in these states do not divide and die, we must assume the percent occupancy of these states is near zero.

If $\Theta_{1,1} \gg 1$, $\Theta_{1,m} \ll 1$ ($m \in \{2 \dots h_1 - 1\}$) and $\Theta_{2,1} \gg 1$, $\Theta_{2,m'} \ll 1$ ($m' \in \{2 \dots h_2 - 1\}$), we get $U^T \approx [U]$, i.e., the populations of all intermediate states are ≈ 0 . Now consider cell state A_1 and all of its intermediate states between cell state $A_{1,2}$. Similar to above, we have

$$A_1^T \equiv [A_1] + \sum_{m=1}^{h_2-1} [C_{13}^m] \quad (59)$$

and

$$A_1^T = [A_1] \left(1 + \frac{\alpha[d_2]}{\Theta_{2,1}} + \frac{[\alpha_1 d_2]^2}{\Theta_{2,1} \Theta_{2,2}} + \dots + \frac{[\alpha_1 d_2]^{h_2-1}}{\prod_{m=1}^{h_2-1} \Theta_{2,m}} \right). \quad (60)$$

Thus, as before, if $\Theta_{2,1} \gg 1$ and $\Theta_{2,m} \ll 1$ ($m \in \{2 \dots h_2 - 1\}$) we have $A_1^T \approx [A_1]$. However, from (45) we also have

$$\begin{aligned} [A_1] &= \frac{[d_1]}{\Theta_{1,h_1}} [C_{01}^{h_1-1}] \\ &= \frac{[d_1]^{h_1}}{\Theta_{1,1} \Theta_{1,2} \dots \Theta_{1,h_1}}. \end{aligned} \quad (61)$$

Since, from above, $\Theta_{1,1} \gg 1$ and $\Theta_{1,m} \ll 1$ ($m \in \{2 \dots h_1 - 1\}$), in order to ensure that $[A_1] \not\approx 0$ we must require that $\Theta_{1,h_1} \ll 1$, in order to offset the large value of $\Theta_{1,1}$, and that $\Theta_{1,m} \gg 1$ ($m \in \{2 \dots h_1 - 1\}$). The latter condition means that $\Theta_{1,m} \approx 1$ ($m \in \{2 \dots h_1 - 1\}$). Therefore, we have the condition that $\Theta_{1,1} \gg \Theta_{1,2} \approx \dots \approx \Theta_{1,h_1-1} \gg \Theta_{1,h_1}$. Similarly, we can derive that $\Theta_{2,1} \gg \Theta_{2,2} \approx \dots \approx \Theta_{2,h_2-1} \gg \Theta_{2,h_2}$ by considering cell state A_2 and all of its intermediate states between cell state $A_{1,2}$ (not shown).

3.4 Generalized derivation without assuming detailed balance

More generally if we do not assume detailed balance, but assume the transition rates between states is much faster than the proliferation of each state (ie $\max(E_0, E_1, E_2, E_3) \ll \min(r_1, r_{-1}, r_2, r_{-2})$), the state occupancy of $U, A_1, A_2, A_{1,2}$ are defined by the partial equilibrium equations

$$\frac{dU}{dt} = -U \cdot (r_1 d_1 + r_2 d_2) + A_1 \cdot r_{-1} + A_2 \cdot r_{-2} \quad (62)$$

$$\frac{dA_1}{dt} = -A_1 \cdot (r_{-1} + \alpha_1 r_2 d_2) + U \cdot r_1 d_1 + A_{1,2} \cdot r_{-2} \quad (63)$$

$$\frac{dA_2}{dt} = -A_2 \cdot (\alpha_2 r_1 d_1 + r_{-2}) + U \cdot r_2 d_2 + A_{1,2} \cdot r_{-1} \quad (64)$$

$$\frac{dA_{1,2}}{dt} = -A_{1,2} \cdot (r_{-1} + r_{-2}) + A_1 \cdot \alpha_1 r_2 d_2 + A_2 \cdot \alpha_2 r_1 d_1 \quad (65)$$

A final constraint is given by the fact that we have assumed slow rate of change of all populations, giving

$$U + A_1 + A_2 + A_{1,2} = C_T. \quad (66)$$

At equilibrium, the equations 62 through 65 must be equal to zero; however, the system only defines a rank 3 matrix, necessitating equation 66. Thus we find

$$\begin{bmatrix} -(r_1 d_1 + r_2 d_2) & r_{-1} & r_{-2} & 0 \\ r_1 d_1 & -(r_{-1} + r_2(\alpha_1 d_2)) & 0 & r_{-2} \\ r_2 d_2 & 0 & -(r_1(\alpha_2 d_1) + r_{-2}) & r_{-1} \\ 1 & 1 & 1 & 1 \end{bmatrix} \cdot \begin{bmatrix} U \\ A_1 \\ A_2 \\ A_{1,2} \end{bmatrix} = \begin{bmatrix} 0 \\ 0 \\ 0 \\ C_T \end{bmatrix} \quad (67)$$

Equations of the form

$$A \cdot \vec{x} = \vec{b}$$

can be solved as

$$\vec{x} = A^{-1} \cdot \vec{b}$$

Furthermore, for a population of cells, it can be easily shown that the net proliferation rate is equal to the average of the entire population. Thus we find

$$E = \begin{bmatrix} E_0 & E_1 & E_2 & E_3 \end{bmatrix} \cdot A^{-1} \cdot \begin{bmatrix} 0 \\ 0 \\ 0 \\ 1 \end{bmatrix} \quad (68)$$

This is derived assuming mass action from the reaction rules $U + d \rightarrow A_1 + d$, $A_1 \rightarrow U$. If instead we assume a multi-step transition as in section *Four-state model with multiple steps between states*, we can simply replace the following in 68

$$\begin{aligned} d_1 &\rightarrow d_1^{h_1} \\ d_2 &\rightarrow d_2^{h_2} \\ \alpha_2 d_1 &\rightarrow (\alpha_2 d_1)^{h_1} \\ \alpha_1 d_2 &\rightarrow (\alpha_1 d_2)^{h_2} \end{aligned}$$

Equation 68 has the following twelve explicit parameters: $r_1, r_{-1}, r_2, r_{-2}, E_0, E_1, E_2, E_3, h_1, h_2, \alpha_1$ and α_2 . There is a relationship defined between a drug's EC_{50} (C in our derivation) and r_1, r_{-1} , and h_1 , given by $EC_{50}^{h_1} = \frac{r_{-1}}{r_1}$.

4 Supplemental Bibliography

References

- BLISS, C. I. (1939). THE TOXICITY OF POISONS APPLIED JOINTLY1. *Annals of Applied Biology*, 26(3):585–615.
- Chou, T.-C. (2010). Drug Combination Studies and Their Synergy Quantification Using the Chou-Talalay Method. *Cancer Research*, 70(2):440–446.
- Chou, T. C. and Talalay, P. (1984). Quantitative analysis of dose-effect relationships: the combined effects of multiple drugs or enzyme inhibitors. *Advances in enzyme regulation*, 22:27–55.
- Chou, T.-C., Talalay, P., Bowie, M., Chou, T.-C., Budinger, J., Watanabe, K., Fox, J., and Philips, F. (1983). Analysis of combined drug effects: a new look at a very old problem. *Trends in Pharmacological Sciences*, 4:450–454.
- Fallahi-Sichani, M., Honarnejad, S., Heiser, L. M., Gray, J. W., and Sorger, P. K. (2013). Metrics other than potency reveal systematic variation in responses to cancer drugs. *Nature Chemical Biology*, 9(11):708–714.
- Greco, W. R., Bravo, G., and Parsons, J. C. (1995). The search for synergy: a critical review from a response surface perspective. *Pharmacological reviews*, 47(2):331–85.
- Loewe, S. (1926). über Kombination swirkungen. *Arch fur Exp Pathology*, 114:313–326.
- Loewe, S. (1927). Versuch einer allgemeinen Pharmakologie der Arznei- kombinationen. *Klinische Wochenschrift*, 6(23):1078–1085.
- Schindler, M. (2017). Theory of synergistic effects: Hill-type response surfaces as ‘null-interaction’ models for mixtures. *Theoretical Biology and Medical Modelling*, 14(1):15.

- Subramanian, A., Narayan, R., Corsello, S. M., Peck, D. D., Natoli, T. E., Lu, X., Gould, J., Davis, J. F., Tubelli, A. A., Asiedu, J. K., Lahr, D. L., Hirschman, J. E., Liu, Z., Donahue, M., Julian, B., Khan, M., Wadden, D., Smith, I. C., Lam, D., Liberzon, A., Toder, C., Bagul, M., Orzechowski, M., Enache, O. M., Piccioni, F., Johnson, S. A., Lyons, N. J., Berger, A. H., Shamji, A. F., Brooks, A. N., Vrcic, A., Flynn, C., Rosains, J., Takeda, D. Y., Hu, R., Davison, D., Lamb, J., Ardlie, K., Hogstrom, L., Greenside, P., Gray, N. S., Clemons, P. A., Silver, S., Wu, X., Zhao, W.-N., Read-Button, W., Wu, X., Haggarty, S. J., Ronco, L. V., Boehm, J. S., Schreiber, S. L., Doench, J. G., Bittker, J. A., Root, D. E., Wong, B., and Golub, T. R. (2017). A Next Generation Connectivity Map: L1000 Platform and the First 1,000,000 Profiles. *Cell*, 171(6):1437–1452.
- Twarog, N. R., Stewart, E., Hammill, C. V., and A. Shelat, A. (2016). BRAID: A Unifying Paradigm for the Analysis of Combined Drug Action. *Scientific Reports*, 6(1):25523.
- Yadav, B., Wennerberg, K., Aittokallio, T., and Tang, J. (2015). Searching for Drug Synergy in Complex Dose–Response Landscapes Using an Interaction Potency Model. *Computational and Structural Biotechnology Journal*, 13:504–513.
- Zimmer, A., Katzir, I., Dekel, E., Mayo, A. E., and Alon, U. (2016). Prediction of multidimensional drug dose responses based on measurements of drug pairs. *Proceedings of the National Academy of Sciences of the United States of America*, 113(37):10442–7.